Ignition of single coal particles in high-temperature oxidizers with various oxygen concentrations

Anna Ponzio [a,*], Sivalingam Senthoorselvan [a,1], Weihong Yang [a], Wlodzmierz Blasiak [a], Ola Eriksson [b]

[a] *School of Industrial Engineering and Management, Royal Institute of Technology, Stockholm, Sweden*
[b] *LKAB, Kiruna, Sweden*

Abstract

In this investigation, coal pellets were combusted using a high temperature oxidizer with varying oxygen concentration, using a small scale batch reactor able to preheat the oxidizer to 1273 K. In base of the experimental results, the influence of oxygen concentration on the ignition mechanism, the solid temperature inside the particle at the moment of ignition, the mass lost at the moment of the ignition and ignition time is analyzed and discussed. A theoretical basis for the division of the conditions tested into three ignition regimes is developed and a formula for the prediction of the ignition time directly from the material and oxidizer temperature and oxygen concentration is proposed.
© 2007 Elsevier Ltd. All rights reserved.

1. Introduction

Combustion of fossil fuels under the condition of high-temperature and low-oxygen concentration has proved to have many features superior to those of conventional combustion [1–10]. For example, the combustion is spread over a larger volume leading to lower peak temperatures and a scarcely visible flame. This phenomenon is referred to as Flameless Oxidation – FLOX [1]. Combustion in high temperature and low-oxygen concentration can also achieve significant energy saving if the combustion air is preheated to temperatures as high as 1273 K, by means of modern regenerative heat exchangers. This technique is referred to as high-temperature air combustion – HiTAC [2]. Since

the temperature increase in the flame in this case is small, it is also called MILD combustion [3]. The HiTAC technology has been developed with the focus primarily on gaseous fuels. Thus, many studies have been performed on the combustion behavior of gaseous fuels under high-temperature and oxygen-deficient conditions by both experimental [2,4–7] and numerical studies [8–10]. A recent development of the technology, called Flameless Oxyfuel [11], is using pure oxygen instead of air and has been successful applied in steel industries [12] with all the benefits of flameless air combustion.

The use of high-temperature oxidizers has been further developed for the biomass gasification processing. In this application, referred to as high-temperature agent gasification (HiTAG), a highly preheated oxidizer with a temperature as high as 1273 K, provides additional energy into the gasification process, which enhances the thermal decomposition of the gasified solids. HiTAG has significant advantages in the gasification of low-rank biomass fuels and traditionally unusable waste streams, like for example

* Corresponding author. Tel.: +46 8 790 8402; fax: +46 8 20 76 81.
E-mail addresses: annaj@mse.kth.se (A. Ponzio), Weihong@mse.kth.se (W. Yang).
[1] Present address: Institute of Energy Systems, Technische Universität München, Germany.

Nomenclature

A	surface area, m^2
c	specific heat capacity, J kg^{-1} K^{-1}
C_1–C_5	constants, defined in Table 3
E	activation energy, J mol^{-1}
h	heat transfer coefficient, J m^{-2} s^{-1}
ΔH	heat of reaction, J mol^{-1}
k	thermal conductivity, W m^{-1} K^{-1}
k_0	rate constant
L	characteristic length, m
K_1–K_2	constants, defined in Table 3
m	mass, kg
$M, \bar{M}$	molar mass, average molar mass, kg/mol
$\dot{n}$	molar flow [mol/s]
Nu	Nusselt number
P	pressure, Pa
Pr	Prandtl number
R	rate of reaction, kg s^{-1}
R	gas constant, J mol^{-1} K^{-1}
Re	Reynolds number
$t, \bar{t}$	time, average time, s
T	temperature, K
Q	heat power, W
V	volume, m^3
x	molar fraction
y	mass fraction

Greek symbols

α	reaction order with respect to oxygen
β	dimensionless constant
γ	reaction order with respect to volatiles
ϕ	dimensionless energy
θ	dimensionless temperature
ρ	density, kg m^{-3}
τ	dimensionless time

Subscripts

p	particle
oxd	oxidizer
ign	ignition
$t = 0$	at time, $t = 0$, i.e. when the sample is inserted into the hot atmosphere
het, coal	heterogeneous combustion of non-devolatilised coal
het, char	heterogeneous combustion of char
hom, vol	homogeneous combustion of volatiles
devol	devolatilisation
vol	volatiles
O$_2$	oxygen

Definition of dimensionless factors

$$\theta = T \cdot \frac{R}{E}$$

$$\phi = \frac{Q}{Ak_0 \Delta H x^\alpha}$$

$$\tau = \frac{kt}{\rho c L^2}$$

as sludge. It can also operate efficiently on a wide range of feedstock [13–16] and the HiTAG gasifier system can be built extremely compact with atmospheric pressure, lowering component costs [13–16]. The state-of-art of high-temperature air-blown gasification technology development has been reviewed by Pian [17]. The modeling work of the HiTAG [18] has shown that based on the agent temperature, two distinct ignition modes are identified: the reaction-controlled and convective-controlled modes.

When the use of high-temperature oxidizers is applied to combustion of pulverized coal, the same advantages as for gaseous fuel can be expected. The advantages include enhancement of combustion stability, increase of combustion efficiency and lower emission of pollutants. Further, the technology can be expected to adapt well to the use of low-volatile coal like anthracite. Some attempts have been carried out to study this concept [19–21]. The results from IFRF [19] reported that the temperature rise in tested furnace with pulverized coal combustion between air inlet and peak in-flame temperature is as low as 150 °C. The measured heat fluxes were high and evenly distributed. It was observed that the intensive entrainment of combustion products into the fuel jets prior to mixing with the air

stream resulted in a very low NO$_x$ emission. Kiga et al. [20] presented the results of pulverized coal combustion in the condition of high-temperature and low-oxygen concentration. They found that a decrease in the oxygen content of the oxidizer lead to a large reduction in the combustion efficiency, and only slight changes of the NO$_x$ emission. Still, their results showed that using the high-temperature air for the combustion of pulverized coal is beneficial. Suda et al. [21] studied the combustion behavior of pulverized coal in high-temperature air, focusing on the effect of air temperature. They reported decreased ignition delays, limited rise in flame temperature, improved coal burnout and decreased NO$_x$ emissions as a result of increased air temperature.

The positive results obtained in previous studies motivate further investigations of coal combustion in high-temperature oxidizers of varying oxygen concentration. One aspect that is particularly interesting is the ignition. It is in fact well known that the ignition behavior of coal is not a material property, but depends strongly on the surrounding conditions. The surrounding conditions in the case of highly preheated oxidizers are indeed extreme and it is thus of interests to understand how ignition behavior

and ignition time depend on the temperature and oxygen concentration of the oxidizer.

The aim of this work is to experimentally study the ignition behavior of coal particles during high-temperature combustion using different oxygen concentrations.

Bituminous coal particles, pellets with a diameter equal to 15 mm, were inserted into high-temperature oxidizers of different oxygen concentration, with the temperature ranging from 873 to 1273 K, and the oxygen concentration ranging from 0% to 100%. The visual ignition phenomenon is described and the dependence of solid temperature, mass loss and ignition time is given. Additionally, in base of the results, theoretical criterions for transition between different mechanisms of ignition in base of the oxidizer temperature and oxygen concentration are derived. Thermal Explosion Theory – TET analysis and heat transfer theory are combined in order to propose a simple formula for the prediction of the ignition time from oxidizer temperature and the predictions are validated by experimental data.

2. Methods and materials

2.1. Feedstock

The experiments in this work used coal pellets made from coal powder and binder (PVC in 20% aqueous solution). The coal powder and binder was mixed in a propor-

tion of 1–0.06 (mass) and pressed in a die with a hydraulic hand press until a pressure of 35 atm to the piston was reached. The resulting cylindrical pellets had a diameter of 15 mm, a height of around 35 mm and a mass of 6.8–6.9 g. The ultimate and proximate analysis of the coal powder used is presented in Table 1.

2.2. Test facility and experimental procedure

Before the experiments started, the pellet was weighted on a precision scale and attached to a piston by means with thin metal wires. A thermocouple was inserted into a hole drilled radially into the pellet at an approximate depth of 1/2 of the diameter in order to measure the solid temperature during the process. A schematic representation of the test facility used in is shown in Fig. 1. The rig consists of a horizontal combustion chamber with an inner diameter about 0.1 m. During the heating stage, propane and air were fed via nozzles (1 and 2) to the gas burner (3). The fuel burned in the combustion chamber (4) and the hot flue gases heated the ceramic honeycomb (5) and flowed through the second part of the reactor (6) and towards the facility's outlet (7). The rig was run in heating mode until the desired temperature of the honeycomb was reached. Once the proper temperature was reached, the fuel feed was shut off and the experimental stage started. The proper oxidizer composition was set by adjusting the flows of air and oxygen or nitrogen and the resulting oxidizer was fed through the air nozzle (2) and was heated by the hot honeycomb (5). The oxidizer temperature was measured by a thermocouple (12). The lid (8) with the piston and the pellet was attached to the rig, with the pellet in a small cooling chamber (9) where it was constantly cooled by nitrogen (10). The experiment started when the pellet on the piston was pushed down into the reactor chamber (6) from above. Once the pellet was in the combustion chamber, the pellet was visible

Table 1
Coal powder properties

Proximate analysis (as received)		Ultimate analysis (dry composition)		
Moisture content	6.7%	Carbon	C	76.0%
Ash content	11.1%	Hydrogen	H	4.0%
LHV	27.99 MJ/kg	Nitrogen	N	1.5%
Volatile matter	19.4%	Oxygen	O	6.2%
Sulphur	0.32%	Chlorine	Cl	<0.01% (wet)
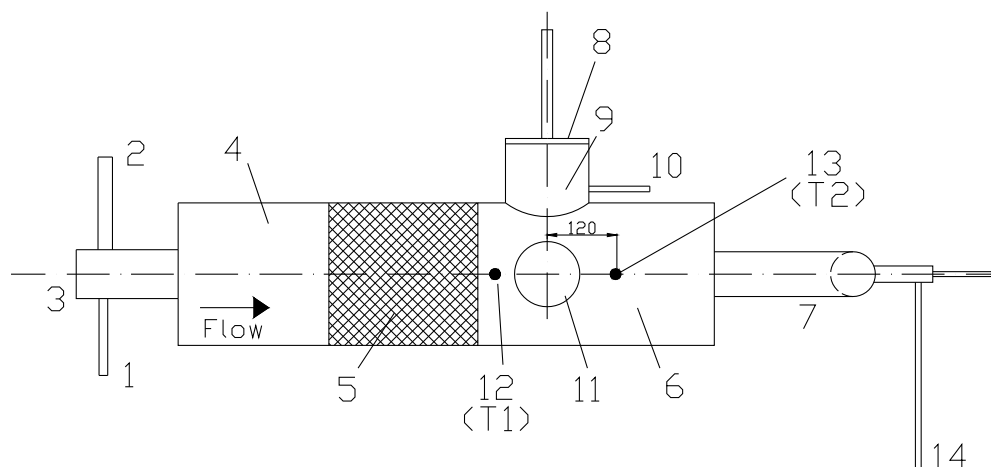
1. Propane nozzle 2. Air/Oxidizer nozzle, 3. Burner, 4. Combustion chamber, 5. Ceramic honeycomb, 6. Reactor chamber, 7. Outlet, 8. Lid, 9. Cooling chamber, 10. Cooling nitrogen nozzle, 11. Glass window, 12. Thermocouple,13 Thermocouple, 14. Product gas sampling. T1 = Oxidizer temperature = T_{oxd}, T2 = flame temperature (not discussed in this paper).

Fig. 1. Schematic picture of the batch type HiTAC/G facility at KTH.

through glass window (11). Through the glass widow (11), the process was recorded by a digital camera. The temperature after the basket was measured by a thermocouple (13). After a certain time (measured by stopwatch), the basket was lifted from the combustion chamber to the cooling chamber (9) in order to quench the reactions through cooling with nitrogen. The pellet was kept in the cooling chamber for 5 min and was then removed from the rig and weighted.

2.3. Data collection and processing

The signals from the thermocouples were collected every 5 s. The heating rate of the coal pellet was estimated by differentiation of the collected temperature curve. The error committed in doing so was estimated to be <10% (computed by comparing a sampling time of 5 s to a sampling time of 15 s). Mass as function of time was reconstructed by weighing samples combusted under identical conditions but in experiment of different duration (1–8 min). The mass loss at a particular time was estimated by assuming a linear mass loss between the measured points. The error in these values was estimated to be <3%, (computed by comparing measured values to those computed from the adjacent points under the assumption of linearity).

The ignition time was measured by stopwatch (using the video recordings of the experiment). The precision in these measurements was around 1 s, due to the fact that the exact insertion time of the sample was difficult to establish precisely (the insertion procedure was manual). Thus, for extremely fast ignitions, for example, for the cases of oxidizer temperature equal to 1273 K and/or oxygen concentrations of 0.30–1.00 (molar basis), the ignition time is given as <1 s without any attempt to precise ignition time further. The temperature at ignition, the heating rate at ignition and the mass loss at ignition are taken as if the ignition time decreased linearly from 1 to 0.25 s when the oxygen concentration increases for those cases. The main

source of error in the ignition time measurements is however believed to be the difficulty to accurately individuate the ignition visually for low temperatures and low-oxygen concentrations.

2.4. Experimental conditions

The experimental conditions are presented in Table 2. In order to reconstruct the mass loss as function of time, several experiments were performed for identical conditions but different duration (time between sample insertion and quenching). A total of 95 experiments were performed, including repetitions.

3. Results and discussion

3.1. Phenomena observed

In Fig. 2 photos taken of the coal pellet at the moment of ignition are presented. By ignition in this case is intended *the first visible sign of combustion*. The photos are ordered from left to right by increasing oxidizer temperature and from top to bottom by increasing oxygen concentration.

When the oxygen concentration and the oxidizer temperature were low, namely 873 K and below or equal to 0.30, the first visible sign of combustion was an orange glowing of the particle surface facing the hot oxidizer. The observed phenomenon was interpreted as *heterogeneous ignition of char* and implies that at least the outer layers of the particle were devolatilised prior to the ignition. Evidently, it took too long time to create flammable conditions in the gas phase for the particle to ignite by development of a flame when the oxygen concentration and the oxidizer temperature were relatively low. Char ignition proceeding the development of a flame, has previously been reported for both coal [22] and wood [23]. In all the cases ignited by a glowing combustion of char (corresponding to the experimental conditions $T_{oxd} = 873$ K and $x_{O_2} = 0.05$–0.30), a yellow flame developed, some time after the initial surface glowing of the particle. The development of the flame started downstream from the particle in the cases $x_{O_2} = 0.05$–0.10 and at the front surface of the particle in the cases $x_{O_2} = 0.21$–0.30. Once the flame appeared, it was no longer possible to observe the weak glowing of the coal particle in the more diluted cases ($x_{O_2} = 0.05$–0.10). Only after the flame extinguished, the glowing of the particle was again observable. This behavior is typical in more diluted conditions where the solid is shielded from oxygen during the flaming phase and char reignition occurs only once the volatile flame extinguishes. The combustion of the coal particle in these cases thus involved three stages: heterogeneous ignition of char (Stage 1), followed by development of a flame (Stage 2) followed by reignition of char once the particle was completely devolatalised (Stage 3).

When the oxidizer temperature was increased to 1073 and 1273 K and the oxygen concentrations kept below or equal to 0.21, the first visible sign of combustion was the

Table 2
Experimental conditions for the experiments with coal particles

| Oxidizer temperature	Oxygen concentration in oxidizer						
	100%	80%	50%	30%	21%	10%	5%
1273 K	1 min	1 min	1 min	1 min	1 min	1 min	1 min
	3 min	3 min	3 min	3 min	2 min	2 min	2 min
					3 min	3 min	3 min
					4 min	4 min	4 min
					5 min	5 min	5 min
	5 min	5 min	5 min	5 min	8 min	8 min	8 min
1073 K	1 min	1 min	1 min	1 min	1 min	1 min	1 min
	3 min	3 min	3 min	3 min	2 min	2 min	2 min
	5 min	5 min	5 min	5 min	3 min	3 min	3 min
					4 min	4 min	4 min
					5 min	5 min	5 min
					8 min	8 min	8 min
873 K	1 min	1 min	1 min	1 min	3 min	3 min	3 min
	3 min	3 min	3 min	3 min	5 min	5 min	5 min
	5 min	5 min	5 min	5 min	8 min	8 min	8 min
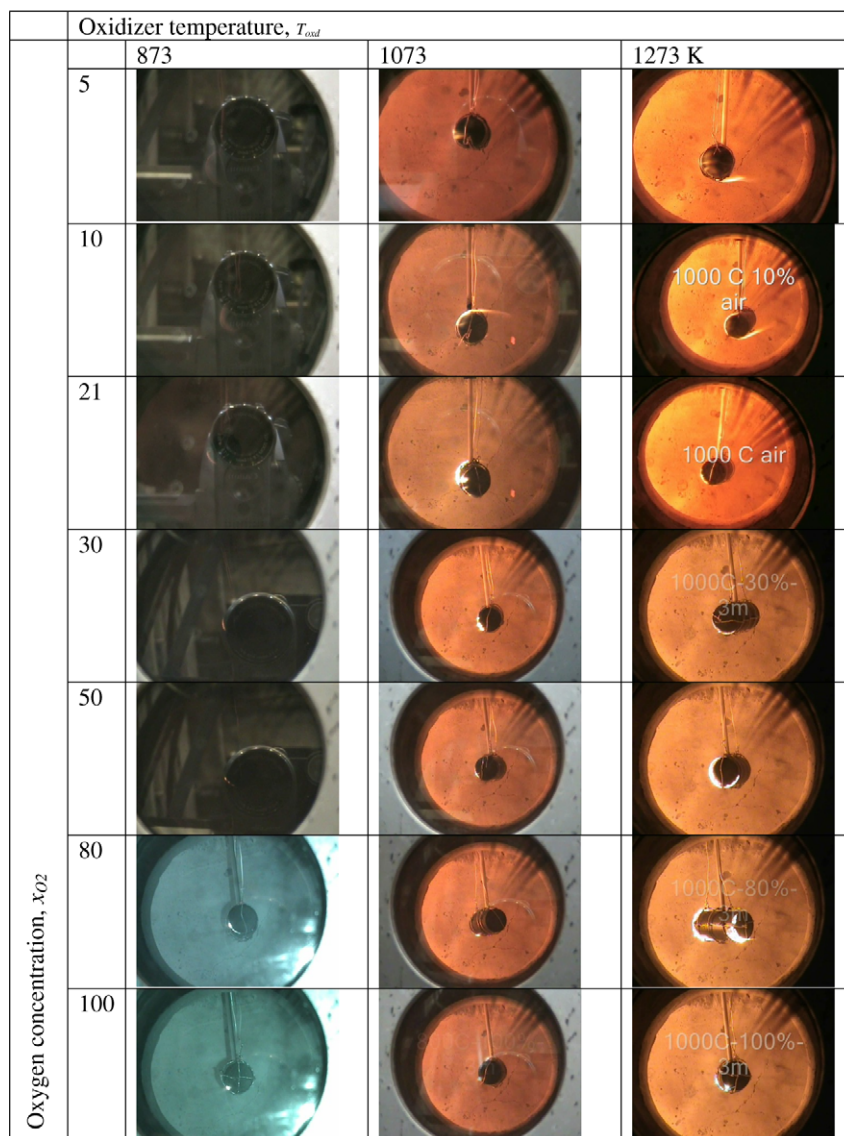
Fig. 2. Picture of the coal particles at the moment of ignition.

development of a flame. Thus the coal particle in these cases was subjected to a *homogeneous ignition of volatiles.* The homogenous mechanism for ignition is well known and was first presented by Faraday, in the middle of the 19th century [24]. The flame started to develop close to the surface on the side of the particle facing the hot oxidizer flow and progressively grew larger. As for the case of oxidizer temperature equal to 873 K and oxygen concentrations below 0.30, a necessary condition for the ignition was that the coal particle started to devolatalise before ignition occurred. In the high temperatures (1073–1273 K), well above the autoignition temperatures of common volatile species like paraffines and carbon monoxide, flammable conditions were apparently created in the boundary layer before the superficial char layer was oxidized at an appreciable rate. Once the flame developed it persisted for significant time and then extinguished. During the entire flaming phase, there was no visible glowing of the particle inside the

flame for the cases $T_{oxd} = 873$–1273 K, $x_{O_2} = 0.05$–0.10. This was probably, again, a manifestation of volatile combustion shielding the forming char from oxygen. Once the volatile flame extinguished, the remaining particle glowed intensely, presumably due to char reignition. The process could thus be said to two-staged: ignition by development of a flame (Stage 1) followed by reignition of char once the particle was completely devolatalised (Stage 2). For slightly higher oxygen concentration, the particle seemed to glow inside the flame, possibly a sign of the flaming combustion and the surface combustion not being mutually exclusive.

Regardless of oxidizer temperature, the same type of ignition phenomenon was observed for high oxygen concentrations ($T_{oxd} = 873$ K–$x_{O_2} = 0.50$–1.00 and $T_{oxd} = 1073$–1273 K–$x_{O_2} = 0.30$–1.00), as can be seen in Fig. 2. The observed ignition was the appearance of small brightly shining sparks in points located on the particle surface (first

visible on the particle edges). The "sparks" progressively grew in number to form a brightly shining layer on the particle surface. The more extreme the conditions (in terms of high oxidizer temperature and high oxygen concentration), the faster the development from single sparks to a "sparking" layer. The interpretation of the phenomena observed was that the particle underwent *heterogeneous ignition of non-devolatilised coal*. By heterogeneous ignition of non devolatilsed coal is intended an attack by oxygen on the whole solid *prior* to devlotalitisation has occurred to a significant extend. The heterogeneous ignition mechanism of non devolatilised coal was first suggested by [25] and is reported to become increasingly important with decreasing particle size [22] and decreasing volatile content [26,27] and has later been suggested also for biomass ignition [28]. The transition towards an increasing importance of heterogeneous reactions in the ignition mechanisms that is predicted by the model developed by Gururajan et al. [29] was here observed experimentally. For the cases with medium oxygen concentration, a flame developed only seconds ($T_{oxd} = 873$ K, $x_{O_2} = 0.50$) or fractions of a second ($T_{oxd} = 1073$–1273 K, $x_{O_2} = 0.30$–0.50) after the heterogeneous attack on the non-devolatilised coal. An intense glowing/sparking of the particle and a volatile flame were visibly observable contemporarily during the flaming period, which means that there were enough oxygen for homogeneous and heterogeneous oxidation not to be mutually exclusive. For the most extreme conditions subjected to a heterogenous ignition of the coal, i.e. cases $T_{oxd} = 873$–1273 K, $x_{O_2} = 0.80$–1.00, no traditional volatile flame developed. Instead, a very intense sparking layer was observed on the front side of the particle while volatiles burned in small local flames on the back side of the particle. Once the small flames on the back side extinguished, this side of the particle started to glow intensively but not "sparkingly" as the front side. The behavior (to show no "traditional" volatile flame but only intense sparking/glowing on the front side and small local flames on the back side of the particle), supports the hypothesis that the available oxygen attacks the coal matrix and combust *on the surface* also material that would else have been expelled as volatiles while only small amounts of volatiles manage to escape from the back side of the particle. The char created by the devolatilisation of the particle's back side was then combusted glowingly in contrast to the sparkling front side. There were thus no clear stages during the combustion in these conditions, and surface oxidation, devolatilisation and volatile combustion appeared to occur more or less contemporarily.

Fig. 3 shows the ignition behavior for the cases where the ignition mechanism started to transit from heterogeneous ignition of char to heterogeneous ignition of non-devolatilised coal (cases $T_{oxd} = 873$ K, $x_{O_2} = 0.30, 0.50$) and from homogeneous ignition of volatiles to heterogeneous ignition of coal (cases $T_{oxd} = 1073$ K, $x_{O_2} = 0.10, 0.21, 0.30$ and cases $T_{oxd} = 1273$ K, $x_{O_2} = 0.05, 0.10, 0.21$). In each case the ignition mechanism is shown by five

photographic shots taken every 0.08 s, every 0.16 s or every 0.32 s from the instant of ignition and on.

The ignition mechanism transited from heterogeneous ignition of char to heterogeneous ignition of non-devolatilised coal when the oxygen concentration was increased above 0.30 in a 873 K oxidizer. The first visual manifestation of the transition was small sparks located in points on the orange glowing surface, visible shortly after the ignition. This occurred already at $x_{O_2} = 0.30$, but only at $x_{O_2} = 0.50$, the sparks were the first sign of combustion, before any glowing was observed.

The ignition transited from a homogeneous ignition of volatiles, to a heterogeneous ignition of non-devolatilised coal when the oxygen concentration was increased around 0.21 in a 1073 K oxidizer or a 1273 K oxidizer. Again, the fist visible sign of the transition was the appearance of small sparks in a thin diffusion flame located on the front side of the pellet. The impression was however that the transition occurred for lower concentrations of oxygen at 1273 K with respect to 1073 K. As was pointed out by Molina and Shaddix [31], it may be tricky to distinguish visually a heterogeneous ignition from the development of a micro-diffusion flame and, therefore, one should be careful to exactly state where the transition occurs. Further, it should be pointed out that the formation of the small sparks and the subsequent development of a diffusion flame close to the surface were almost inseparable for high temperatures, 1073–1273 K, and medium to high oxygen concentrations (0.21–1.00). At an oxygen concentration of 0.10, the ignition mechanism was, however, clearly homogeneous. At an oxygen concentration of 0.30, ignition was on the contrary clearly occurring by small local sparks on the particle surface – thus by a heterogeneous mechanism – even though a diffusion flame was created only fraction of a second after.

From the results presented in Fig. 3, it can be concluded the transition from heterogeneous ignition of char or homogeneous volatile ignition to a heterogeneous ignition of non-devolatilised coal occurred earlier (i.e. for lower oxygen concentrations) when the temperature of the oxidizer was higher.

The transition from heterogeneous char ignition to homogeneous volatile ignition occurred for oxidizer temperatures somewhere between 873 and 1073 K and only for low-oxygen concentrations (0.05–0.21) for the coal particles and experimental set up in question.

3.2. Solid temperature at the moment of ignition

Fig. 4 shows the temperature inside the coal particle at the moment of ignition. Due to temperature gradients, the temperature measured inside the particle is different from the surface temperature and the discrepancy between the two will be larger the shorter the ignition time. However, the trends in function of the oxidizer temperature and oxygen concentration for the temperatures on the surface and inside the particle will be similar. In fact, it has
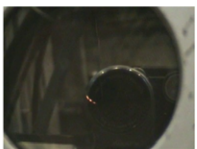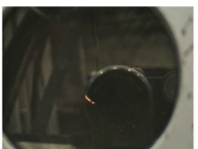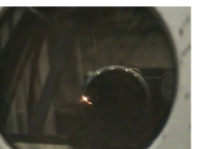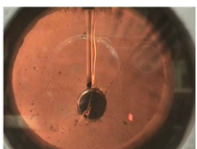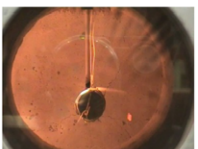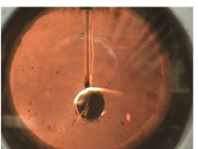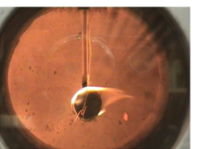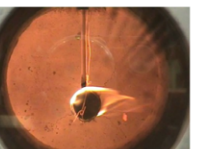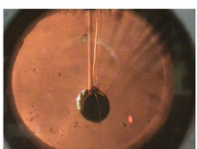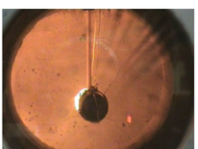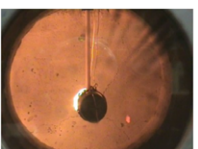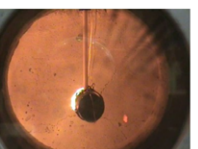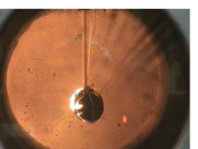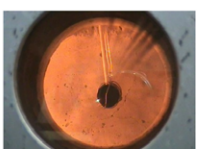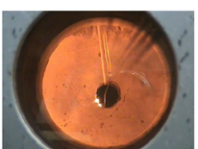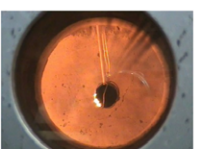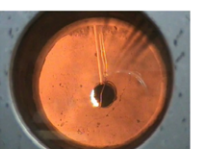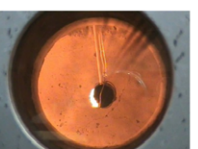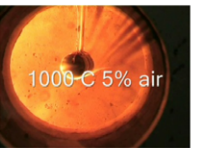
Oxidizer temperature, T_{oxd} = 873 K				
x_O=0.30				
Ign	+0.32s	+0.64s	+0.96s	+1.28s
x_O=0.50				
Ign	+0.16s	+0..32s	+0.48s	+0.64s
Oxidizer temperature, T_{oxd} = 1073 K				
x_O=0.10				
Ign	+0.32s	+0.64s	+0.96s	+1.28s
x_O=0.21				
Ign	+0.32s	+0.64s	+0.96s	+1.28s
x_O=0.30				
Ign	+0.8s	+0.16s	+0.24s	+0.32s
Oxidizer temperature, T_{oxd} = 1273 K				
x_O=0.05				
Ign	+0.32s	+0.64s	+0.96s	+1.28s
x_O=0.10				
Ign	+0.16s	+0..32s	+0.48s	+0.64s
x_O=0.21				
Ign	+0.8s	+0.16s	+0.24s	+0.32s

Fig. 3. Ignition behavior – transition from pyrolysis controlled ignition to direct attack on the coal particle surface.
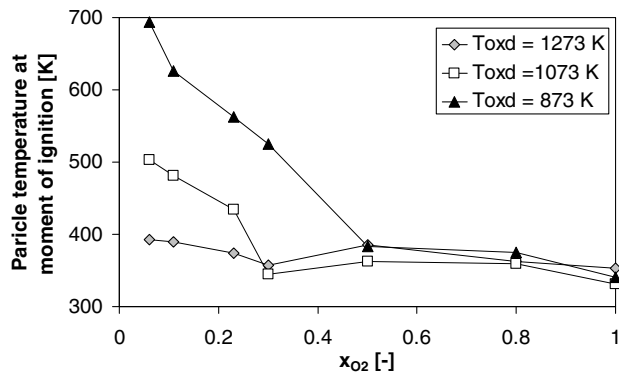
Fig. 4. Solid temperature at the moment of ignition as function of the oxygen concentration in the oxidizer for different oxidizer temperatures.

been shown that the measured "ignition temperature" may vary as much between 500–1300 K in base of the experimental method chosen [22,29] so it is indeed motivated to focus on trends rather then absolute values.

As can be seen, the temperature of the solid at the moment of ignition decreased with increasing oxidizer temperature and increasing oxygen concentration for the cases $T_{oxd} = 873$ K, $x_{O_2} = 0.05–0.30$ and $T_{oxd} = 1073–1273$ K, $x_{O_2} = 0.05–0.21$ whilst it appeared insensitive to both oxygen concentration and oxidizer temperature for the cases $T_{oxd} = 873$ K, $x_{O_2} = 0.50–1.00$ and $T_{oxd} = 1073–1273$ K, $x_{O_2} = 0.30–1.00$.

The trends in Fig. 4, confirm with the ignition phenomena observed visually. Decreasing ignition temperatures with increasing oxygen concentration is predicted by thermal explosion theory for heterogeneous ignition [22] and similar trends has also been reproduced for homogeneous ignition by the model of Gururajan et al. [29]. Gururajan et al. also found that the inclusion of a heterogeneous reaction in their ignition model, increased the oxygen dependence in the range 0.10–0.50. This is in accordance with the observed tendency of more pronounced influence of oxygen concentration for the cases 873 K, $x_{O_2} = 0.05–0.30$ where the mechanism was heterogeneous char ignition, than for the cases 1073 K, $x_{O_2} = 0.05–0.21$ and 1273 K, $x_{O_2} = 0.05–0.21$, where the mechanism is homogeneous.

According to the model developed by Gururajan et al. [29] and thermal explosion theory of heterogeneous ignition [22], the ignition temperature decreases less rapidly with increasing oxygen concentration at high-oxygen concentration (appr. > 0.50). In the experiments performed in this work, the solid temperature at the moment of ignition for the cases subjected to heterogeneous ignition of coal, i.e. $T_{oxd} = 873$ K, $x_{O_2} = 0.50–1.00$ and $T_{oxd} = 1273$ K, $x_{O_2} = 0.30–1.00$, was almost independent of oxygen [Fig. 4]. This may be due the fact that the variations in ignition temperature are within the limits of error for these conditions (remembering that the ignition time was less then 1 s) and that the temperature gradients within the particle are comparatively large at the short ignition times in question (see next paragraph).

Heterogeneous ignition theory predicts the solid temperature to be independent of the oxidizer temperature. This is in perfect accordance with the observation for the cases 873 K, $x_{O_2} = 0.50–1.00$ and 1073–1273 K, $x_{O_2} = 0.30–1.00$ (Fig. 4). On the contrary, experiments with wooden spheres inserted in streams of hot air has shown that the ignition temperature for flaming ignition is indeed inversely dependent on oxidizer temperature [23]. This is in accordance with the trends in Fig. 4 where the solid temperature at the moment of ignition decreases as the temperature of the oxidizer increases for the cases ignited homogeneously i.e. $T_{oxd} = 1073–1273$ K, $x_{O_2} = 0.05–0.21$. The drastic decrease in ignition temperature between the cases 873 K, $x_{O_2} = 0.05–0.30$ on one hand, and the cases 1073–1273 K, $x_{O_2} = 0.05–0.21$ on the other, must in consequence be interpreted as a transition from temperature *independent* heterogeneous char reaction to temperature *dependent* homogeneous volatile ignition. This is also in accordance with [29] who reported the ignition temperature to decrease with increasing tendency to ignite homogenously.

3.3. Mass lost at the moment of ignition

The mass lost from the coal particle at the moment of ignition is presented in Fig. 5.

Generally, very little mass was lost at the moment of ignition: between 0.9 and 3.5% for $T_{oxd} = 873$ K, between 0.3% and 1.4% for $T_{oxd} = 1073$ K and between 0.2% and 0.4% for $T_{oxd} = 1273$ K. This means that the particle at the moment of ignition, regardless the ignition mechanism, was not completely dried and far from completely devolatalised. Two conclusions may thus be drawn: (1) the char layer subjected to the heterogeneous ignition in the cases of low-oxidizer temperature (873 K) and low-oxygen concentrations (0.05–0.30) was relatively thin; and (2) very low concentrations of volatiles are needed to create flammable condition in the boundary layer when high-temperature oxidizers (1073–1273 K) are used, even when the oxygen concentration is relatively low, for example, 0.05. The mass lost at the moment of ignition was the smallest
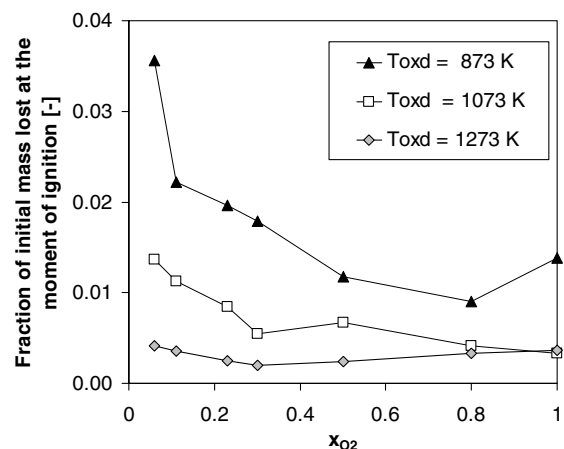

Fig. 5. The mass loss at the ignition.

for the cases $T_{\mathrm{oxd}} = 873$ K, $x_{\mathrm{O_2}} = 0.50$–1.00 and cases $T_{\mathrm{oxd}} = 1073$–1273 K, $x_{\mathrm{O_2}} = (0.21$–$1.00)$ which supports the hypothesis that it is coal rather than char that is attacked heterogeneously by oxygen at the moment of ignition under these conditions.

3.4. Ignition mechanism in function of oxidizer properties

Above, visual evidence, solid temperature at the moment of ignition and mass lost at the moment of ignition was presented and used to support the classification of the observed ignition behavior under various conditions as three well known ignition mechanisms, i.e.

- Glowing surface ignition by heterogeneous oxidation of char when the oxidizer temperature and the oxygen concentrations were low.
- Flaming ignition by homogeneous ignition of volatiles when the oxidizer temperature was high and the oxygen concentration low.
- Sparking ignition by heterogeneous oxidation of the non devolatalised coal when the oxidizer temperature was high and the oxygen concentration was medium or high.

It is interesting to define theoretical criteria for the mechanism with which a particle will ignite in function of the surrounding conditions. In this way, the ignition mechanism could be predicted directly from the oxygen concentration and the oxidizer temperature, something that may find relevance in design of HiTAC burners and HiTAG gasifiers where a particular ignition mechanism or no ignition at all is desired. Such criteria could be identified by comparing the rates of the involved reactions, namely the rate of heterogeneous oxidation of non devolatalised coal $r_{\mathrm{het,coal}}$, the rate of devolatilisation, r_{devol}, the rate of heterogeneous oxidation of char, $r_{\mathrm{het,char}}$, and the rate of homogeneous oxidation of volatiles, $r_{\mathrm{hom,vol}}$.

Firstly, heterogeneous ignition of char and homogeneous ignition of volatiles are both ignition of devolatilisation products, while heterogeneous ignition of non-devolatilised coal is not. A necessary condition for the ignition of char or volatiles to occur is that the rate of devolatilisation exeeds the rate of oxidization of non-devolatilised coal, i.e. $r_{\mathrm{devol}} > r_{\mathrm{het,coal}}$ during the period prior to the ignition. Vice versa, a necessary condition for the heterogeneous ignition of non-devolatilised coal is that $r_{\mathrm{het,coal}} > r_{\mathrm{devol}}$. Secondly, if the ignition occurs after the sample is devolatilised (i.e if $r_{\mathrm{devol}} > r_{\mathrm{het,coal}}$), it may be either by a homogeneous ignition of the volatiles or by a heterogeneous ignition of the char. If the rate of oxidation of the char surface is larger than the rate of the volatile combustion, ($r_{\mathrm{het,char}} > r_{\mathrm{hom,vol}}$), the particle will ignite by a glowing reaction on the char surface. If the reverse is true, ($r_{\mathrm{hom,vol}} > r_{\mathrm{het,char}}$), the sample will ignite by development of a flame. From the discussion the following regimes can thus be defined:

Ignition regime 1 – heterogeneous ignition of non devolatiled coal: $r_{\mathrm{het,coal}} > r_{\mathrm{devol}}$

Ignition regime 2 – heterogeneous ignition of char: $r_{\mathrm{devol}} > r_{\mathrm{het,coal}}$ and $r_{\mathrm{het,char}} > r_{\mathrm{hom,vol}}$

Ignition regime 3 – homogeneous ignition of volatiles: $r_{\mathrm{devol}} > r_{\mathrm{het,coal}}$ and $r_{\mathrm{hom,vol}} > r_{\mathrm{het,char}}$

Now, the interest is to express the delimitation of these regimes in the relevant key variables, namely oxygen concentration and oxidizer temperature. The critical conditions in terms of oxygen concentration and oxidizer temperature for transition between the different regimes (and corresponding mechanisms) can be found by equaling the involved rates and use the common kinetically expressions for the reaction rates:

Transition between regime 1 on one hand and regimes 2 and 3 on the other

$$r_{\mathrm{het,coal}} = r_{\mathrm{devol}} \tag{1}$$

Transition between regime 2 and regime 3:

$$r_{\mathrm{devol}} > r_{\mathrm{het,coal}} \quad \text{and} \quad r_{\mathrm{hom,vol}} = r_{\mathrm{het,char}} \tag{2}$$

The formula for the rate of devolatilisation rate is taken from [29]

$$r_{\mathrm{devol}} = m_{\mathrm{p}} \cdot y_{\mathrm{vol}} \cdot k_{0,\mathrm{devol}} \cdot \mathrm{e}^{-\frac{E_{\mathrm{devol}}}{RT_{\mathrm{p}}}} \tag{3}$$

The formula for rate of heterogeneous combustion of coal (the whole coal) is taken from [29]

$$r_{\mathrm{het,coal}} = A_{\mathrm{p}} \cdot (p \cdot x_{\mathrm{O_2}})^{\alpha_{\mathrm{het,coal}}} \cdot k_{0,\mathrm{het,coal}} \cdot \mathrm{e}^{-\frac{E_{\mathrm{het,coal}}}{RT_{\mathrm{p}}}} \tag{4}$$

Also for the heterogeneous reaction between oxygen and char, Eq. (4) was used (this time with kinetic constants relative to char instead of coal).

$$r_{\mathrm{het,char}} = A_{\mathrm{p}} \cdot (p \cdot x_{\mathrm{O_2}})^{\alpha_{\mathrm{het,char}}} \cdot k_{0,\mathrm{het,char}} \cdot \mathrm{e}^{-\frac{E_{\mathrm{het,char}}}{RT_{\mathrm{p}}}} \tag{5}$$

The formula for the rate of homogenous combustion of volatiles is taken from [29]

$$r_{\mathrm{hom,vol}} = \bar{M}_{\mathrm{vol}} \cdot \left(\frac{p}{RT_{\mathrm{oxd}}} x_{\mathrm{O_2}} \right)^{\alpha_{\mathrm{hom,vol}}} \cdot \left(\frac{p}{RT_{\mathrm{oxd}}} x_{\mathrm{vol}} \right)^{\gamma}$$
$$\cdot k_{0,\mathrm{hom,vol}} \cdot \mathrm{e}^{-\frac{E_{\mathrm{hom,vol}}}{RT_{\mathrm{oxd}}}} \tag{6}$$

Since the particle is immersed in a continuously flowing gas stream, it is reasonable to assume that the concentration of volatiles in the gas phase is proportional to the devolatilisation rate. The relation for the concentration of volatiles used in Eq. (6) can thus be approximated as:

$$x_{\mathrm{vol}} = \frac{r_{\mathrm{devol}}}{\bar{M}_{\mathrm{vol}} \cdot \dot{n}_{\mathrm{oxd}}} = \frac{m_{\mathrm{p}} \cdot y_{\mathrm{vol}} \cdot k_{0,\mathrm{devol}} \cdot \mathrm{e}^{-\frac{E_{\mathrm{devol}}}{RT_{\mathrm{p}}}}}{\bar{M}_{\mathrm{vol}} \cdot \dot{n}_{\mathrm{oxd}}} \tag{7}$$

In Eqs. (3), (4), (5) and (7), the rate depends on the particle temperature. During the first moments after the insertion of the pellet, the temperature increase of the particle with respect to the temperature at the moment of insertion can be assumed to be proportional to the initial temperature difference between the oxidizer and the particle. Therefore,

the following relationship between particle temperature and oxidizer temperature was used in Eqs. (3), (4), (5) and (7):

$$T_p = C \cdot \frac{A_p \cdot h}{c_p \cdot \rho_p \cdot V_p} \cdot (T_{oxd} - T_{p,t=0}) + T_{p,t=0} \qquad (8)$$

Inserting Eqs. (3)–(8) in to Eqs. (1) and (2) and solving with respect to oxygen concentration, the following new relations between oxygen concentration and oxidizer temperature at transitions between the different ignition regimes (and corresponding mechanisms) are derived:

Critical ambient conditions for transition between heterogeneous ignition of non-devolatilised coal and ignition of devolatilisation products (delimitation between regime 1 on one hand and regimes 2 and 3 on the other):

$$x_{O_2} = \left(\frac{1}{p}\right) \cdot \left(\frac{m_p \cdot y_{vol}}{A_p} \cdot \frac{k_{0,devol}}{k_{0,het,coal}}\right)^{1/\alpha_{het,coal}}$$
$$\cdot \exp\left(-\frac{1}{\alpha_{het,coal}} \frac{\Delta E_1}{R\left(C_1 \cdot \frac{h \cdot A_p}{m_p \cdot c_p}(T_{oxd} - T_{p,t=0}) + T_{p,t=0}\right)}\right) \qquad (9)$$

Critical ambient conditions for transition between heterogeneous ignition of volatiles and homogeneous ignition of volatiles (delimitation between regime 2 and regime 3):

$$x_{O_2} < \left(\frac{1}{p}\right) \cdot \left(\frac{m_p \cdot y_{vol}}{A_p} \cdot K_1\right)^{1/\alpha_{het,coal}} \cdot \exp\left(-\frac{1}{\alpha_{het,coal}} \frac{\Delta E_1}{R\left(C_1 \cdot \frac{h \cdot A_p}{m_p \cdot c_p}(T_{oxd} - T_{p,t=0}) + T_{p,t=0}\right)}\right)$$

and

$$x_{O_2} = const. \cdot f_1(T_{oxd}) \cdot f_2(T_{oxd})$$

$$const. = \frac{1}{p}\left(\frac{\bar{M}_{vol}}{A_p}\right)^{\alpha_{hom,vol}+\gamma} \cdot \left(\frac{1}{R}\right)^{\alpha_{hom,vol}+\gamma} \cdot \left(\frac{p \cdot m_p \cdot y_{vol}}{\dot{n}_{oxd} \cdot \bar{M}_{vol}}\right)^{\gamma} \cdot K_2^{\frac{1}{(\alpha_{het,char} - \alpha_{hom,vol})}}$$

$$f_1(T_{oxd}) = \left(\frac{1}{T_{oxd}}\right)^{\frac{\alpha_{hom,vol}+\gamma}{(\alpha_{het,char} - \alpha_{hom,vol})}}.$$

$$f_2(T_{oxd}) = \left(\exp\left(-\frac{1}{(\alpha_{het,char} - \alpha_{hom,vol})}\right.\right.$$
$$\left.\left.\times\left(\frac{\Delta E_2}{R\left(C_2 \cdot \frac{h \cdot A_p}{m_p \cdot c_p}(T_{oxd} - T_{p,t=0}) + T_{p,t=0}\right)} + \frac{E_{hom,vol}}{R T_{oxd}}\right)\right)\right) \qquad (10)$$

The conditions (9) and (10) represent two lines in the oxygen concentration–oxidizer temperature plane that delimits the three different ignition regimes from each other. They thereby represent a novel tool to determine directly from the oxygen concentration and oxidizer temperature whether the particle will ignite by heterogeneous attack on the non-devolatilised coal, by an attack on the char or through the development of a volatile flame.

In Fig. 6, these lines have been fitted to the observed transitions. The values of the constants and their definition used are presented in Table 3. The negative sign of the ΔE_1 and ΔE_2 implies that the activation energy for heterogeneous combustion of non-devolatilised coal and char is larger than the activation energy for devolatilisation which is
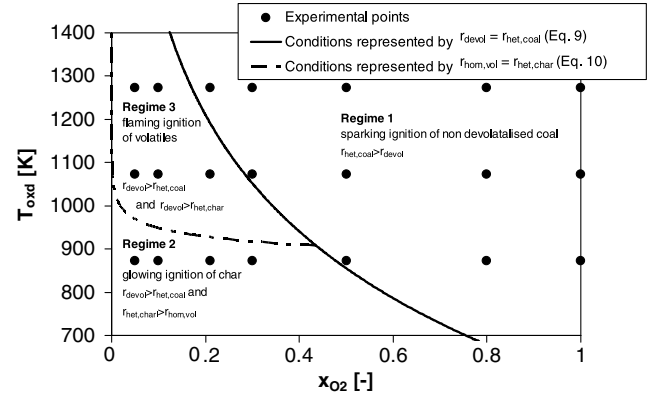

Fig. 6. Ignition regimes for the different experimental conditions tested.

Table 3
Constants used in the formulas for conditions for transition of ignition mechanisms

Constant	Value
$\alpha_{het,coal}$	0.13
$\alpha_{het,har}$	0.13
$\alpha_{hom,vol}$	1.0
γ	1.0
$K_1 = \frac{k_{0,devol}}{k_{0,het,coal}}$	8.8×10^{-3} m^2 Pa$^{0.13}$ kg^{-1}
$\Delta E_1 = (E_{devol} - E_{het,coal})$	-15×10^3 J mol^{-1}
C_1	1.3 s
$K_2 = \frac{k_{0,devol}^{\gamma} \times k_{0,hom,vol}}{k_{0,het,char}}$	2.8×10^{10} m^8 Pa$^{0.13}$ s^{-1} mol^{-1} kg^{-1}
$\Delta E_2 = (\gamma \times E_{devol} - E_{het,char})$	-7.4×10^3 J mol^{-1}
E_{hom}	2.5×10^5 J mol^{-1}
C_2	2 s

Definition and values of the constants used to fit the expression to visually observed transition.

reasonable and in line with other authors. The larger value (in absolute terms) of ΔE_1 indicates that the activation energy of non devolatilised coal is larger than the activation energy of char. This is in accordance with other estimations of kinetic parameters from ignition temperature measurements [30]. The value of the activation energy for volatile combustion is high compared to those used in the model by Gururajan et al. [29]. The reason may be that the composition of the volatiles formed from devolatilisation in highly preheated oxidizers is different.

Naturally, the transitions in reality occur gradually around the identified lines delimiting the ignition regimes. Further, it should be pointed out, that due to the relative uncertainty in the visual identification of ignition mechanism and the relatively low number of experimental points in the critical regimes, the degree of liberty in the choice of the constant values that fit the data is quite large, especially so for relation (10). With certainty, it may, however, be claimed that:

(1) In the case of relation (9), the form of the theoretically derived expression is confirmed by the experi-

mental evidence. The lower the oxidizer temperature, the higher the oxygen concentration required to transit from an ignition of devolatilisation products (volatiles or char) to an ignition of non-devolatilised coal. This was observed visually.

(2) In the case of relation (10), the form of the theoretically derived expression is not contradicted by the experimental evidence. The theory developed predicts the transition from heterogenous ignition of char to homogeneous ignition of volatiles to occur at higher oxidizer temperatures, the lower the oxygen concentration. This is due to the fact that the order of volatile combustion with respect to oxygen was set higher that that of char combustion. To confirm this tendency, more experiments would be needed in the regime.

From the relations (9) and (10) it is clear that the position of the transition in the oxygen concentration–oxidizer temperature plane depend on particle size, coal properties, volatile content, heat transfer rate and kinetics parameters for the involved reactions. These were all parameters assumed to be constant in the performed experiments, but the variation of ignition mechanism with some of some of these properties namely heating rate, particle size and volatile content has been previously reported [22,26,27] and ignition regimes in the heating rate–particle diameter plane has previously been identified [22].

3.5. Ignition time

Fig. 7 shows the measured ignition times as function of the oxygen concentration. In the case of oxidizer temperature 873 K, also the time required to develop a flame after the char/coal ignites heterogeneously is reported. For cases subjected to heterogeneous ignition of coal at higher oxidizer temperatures, i.e. 1073–1273 K, the formation of a flame followed only fractions of a second after the heterogeneous attack and is, therefore, not shown.

As can be seen, the time to ignition varied significantly with oxygen concentration and oxidizer temperature in a way similar to the solid temperature at the moment of ignition. However, the dependence of ignition time on both oxygen concentration and oxidizer temperature was even more pronounced than in the case of solid temperature at the moment of ignition. This is due to the fact that ignition time depends on both the ignition temperature and the heating rate. As was shown above, the ignition temperature increased with decreasing oxygen concentration and decreasing temperature. Obviously, the heating rate will be affected positively by increasing oxidizer temperature and increasing oxygen concentration (by increased heat transfer from the oxidizer and increased heat release by reaction). Thus, the ignition time is even more effected by changes in the oxidizer temperature, than the solid temperature at the moment of ignition. An accelerating effect on coal ignition by increasing oxygen concentration has also

recently been reported by [31]. The reported tendency of char to ignite slower than non devolatilise coal has also support in the literature [32]. In this case, char ignition and coal ignition occurred for different oxygen concentrations which further accentuated this tendency. Yang et al. [33], reported that ignition time decreases rapidly for increasing heat fluxes up to approx. 30 kW/m^2 (a range of relevant to the experiment in this work) and that the differences in ignition times for different ignition temperatures were the largest for low heat fluxes. This is also in accordance with the trends shown in Fig. 7.

3.6. Ignition time as function of the oxidizer properties

The ignition time, i.e the time required for the particle inserted into certain conditions to ignite, is an important variable in combustion applications and fire prevention. In order to predict ignition time, a transient model of some kind is used and the ignition time is taken as the time to reach the ignition temperature. In practice, the ignition temperature is often used as a fuel property. Ignition temperature – and consequently ignition time – does, however, depend strongly on the surrounding conditions. It is interesting to model this dependence. This would be particularly important for HiTAC and HiTAG applications, where the surrounding conditions are quite extreme.

In the time preceding the ignition, it can be assumed that the heat release by reaction can be neglected. The transient temperature of a sufficiently large particle can thus be represented fairly well by heat conduction theory for an infinite solid [23]:

$$\tau_{\text{ign}} = \pi \left(\frac{k_{\text{s}}}{k_{\text{oxd}}} \right)^2 \left(\frac{(\theta_{\text{ign}} - \theta_{\text{p},t=0})}{(\theta_{\text{oxd}} - \theta_{\text{p},t=0})Nu} \right)^2 \tag{11}$$

$$\tau_{\text{ign}} = \frac{k_{\text{p}} t_{\text{ign}}}{\rho_{\text{p}} c_{\text{p}} L_{\text{p}}^2} \tag{12}$$

$$\theta = T \cdot \frac{R}{E} \tag{13}$$

Eq. (11) has been successfully used by Kuo and His [23] to correlate ignition times to measured ignition temperatures for the ignition of wooden spheres in a air streams of 673–873 K. Compared to the thermal explosion theory, the formula has also the advantage of accounting for the thermal inertia of the particle, which is relevant in cases of particle as large as in the experiments performed. In this relation, the ignition temperature – i.e. the solid surface temperature at the moment of ignition appears. However, the formula does not give any information about the ignition criteria used nor how the ignition temperature varies with the surrounding conditions.

In the experimental work presented above, the ignition criteria used was "First visible sign of combustion by glowing, sparking or flame". For the mathematical expression, a numerical ignition criterion is needed. An ignition criterion that applies to the conditions used in this experimental

work is the Chen et al. criterion [34] here applied to the reaction rate given by Eqs. (4) and (5)

$$\begin{cases} \left(\frac{d\phi}{d\theta}\right)_{ign} = 0 = \frac{e^{-1/\theta_{ign}}}{\theta_{ign}^2} - \frac{k_{oxd}E}{k_0\Delta Hp^\alpha L_p R} \cdot \frac{Nu}{x_{O_2}^\alpha} \\ \phi \geqslant 0 \end{cases} \quad (14)$$

where

$$\phi = \frac{Q}{A_p k_0 \Delta Hp^\alpha x_{O_2}^\alpha} \quad (15)$$

The Chen et al. criterion is based on an energy balance of the particle surface and the resulting ignition temperature is a function of fuel properties, reaction kinetics, Nusselt number and oxidizer composition. It should be noted the criteria $\phi \geqslant 0$ in the case of oxidizer temperatures above the ignition temperature of the solid is always respected in the experiments performed since the surroundings heat the particle and not vice versa.

The exponential form makes Eq. (15) tricky to handle. To get rid of the exponent, the following approximation, proposed by Cassel and Liebmann [35] can be used

$$\exp(-1/\theta) \cong C_3 \cdot \theta^\beta \quad (16)$$

With approximation (16), the criteria for ignition according to Chen becomes

$$\theta_{ign} = \left(\frac{k_{oxd} \cdot E}{k_0\Delta Hp^\alpha L_p R} \cdot \frac{1}{C_3}\right)^{\frac{1}{\beta-2}} \cdot \left(\frac{Nu}{x_{O_2}^\alpha}\right)^{\frac{1}{\beta-2}} \quad (17)$$

In Eq. (17), the dependence of the ignition temperature on the oxygen concentration and the Nusselt number is considered. Dependence on the oxidizer temperature is, however, not considered, unless the Nusselt number is used to account also for irradiative effects. This may seem contradictory to the result previously presented. It should be pointed out that the particle temperature was measured inside the particle, and that the variations in surface temperature at the moment of ignition with oxidizer temperature may have been smaller than the variation of the measured temperature (see Fig. 4) due to substantial gradients within the particles. Never the less, the ignition criterion according to Chen et al. fails to account for the dependence of ignition temperature on oxidizer temperature in homogeneous ignition, even though the error may be limited, but is used because of its simplicity.

By the insertion of ignition criterion (17) into Eq. (11) a new formula for prediction of the ignition time in function of the oxygen concentration and oxidizer temperature is derived

$$\tau_{ign} = C_5 \cdot \pi \left(\frac{k_s}{k_{oxd}}\right)^2 \left(\frac{\left(\left(\frac{k_{oxd}\cdot E}{\Delta Hp^\alpha L_p R} \cdot C_4\right)^{\frac{1}{\beta-2}} \cdot \left(\frac{Nu}{x_{O_2}^\alpha}\right)^{\frac{1}{\beta-2}} - \theta_{p,t=0}\right)}{(\theta_{oxd} - \theta_{p,t=0})Nu}\right)^2 \quad (18)$$
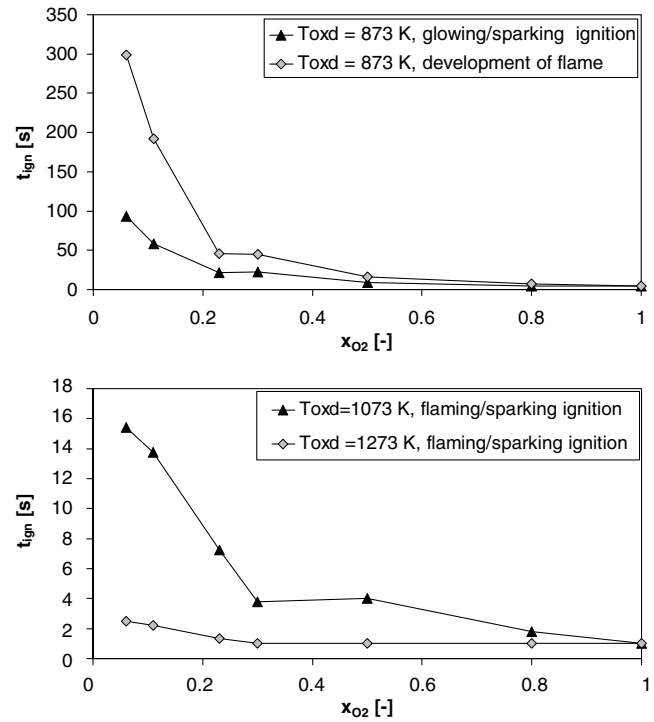
$$C_4 = \frac{1}{k_0 \cdot C_3} \quad (19)$$

Fig. 7. Time to ignition in function of the oxygen concentration.

The Nusselt number is computed according to

$$Nu = \frac{h \cdot L_p}{k_{oxd}} \quad (20)$$

where

$$h = 0.683 Re^{0.466} Pr^{1/3} \frac{k_{oxd}}{L_p} \quad (21)$$

In Eq. (20), α represents the order of the combustion reaction with respect to oxygen. The ratio E/R can be chosen arbitrarily as a normalization factor for the temperature as long as the kinetic behavior of the process is accounted for by the fitting the factor β and the constant C_5 to experimental data.

In Fig. 8, the normalized ignition time is plotted as function of the oxygen concentration, both measured (points) and estimated (curves) using Eq. (18) and the values of the constants specified in Table 4. As can be seen, the kinetic constants used (β and C_4) differ between the cases. The measured values are average values for the experimental cases using as criterion for ignition "first visible sign of combustion by glowing, flame or sparks".

Further, the ignition time for the conditions identified by Eqs. (9) and (10) has been inserted in Fig. 8. The conditions identified by Eqs. (9) and (10) represent the critical conditions for transition between the different ignition regimes discussed in Section 3.4. The ignition time in this case has been computed both using the kinetic constants β and C_4 belonging to the case $T_{oxd} = 1273$ K ($C_4 = 66$ and $\beta = 2.65$) and the case $T_{oxd} = 873$ K ($C_4 = 230$ and $\beta = 2.35$).
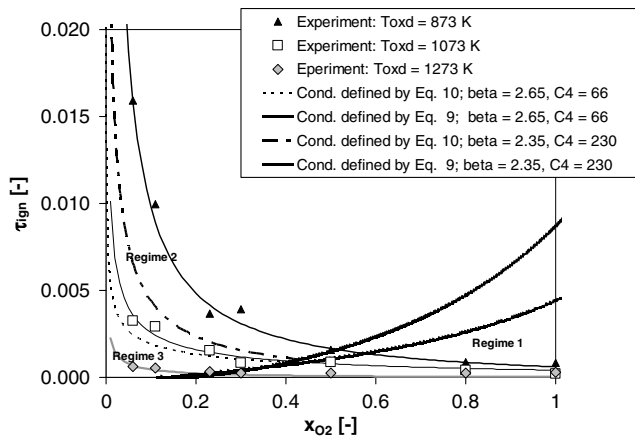
Fig. 8. Dimensionless ignition time in function of the oxygen concentration.

Table 4
Constants used in Eq. (18) for the prediction of the ignition time from oxidizer

	$T_{oxd} = 1273$ K	$T_{oxd} = 1073$ K	$T_{oxd} = 873$ K
C_5	1.6×10^{-3}	1.6×10^{-3}	1.6×10^{-3}
C_4	66	110	230
β	2.7	2.6	2.4
α	0.13	0.13	0.13

As can be seen, Eq. (18) successfully depicts the trends of the ignition time in function of both temperature and oxygen concentration in the oxidizer. Further, it respects the intuitive condition that the ignition time should tend towards infinity as oxygen concentration approaches zero. It is remarkable how well the trends fit even the cases where the ignition is not clearly heterogeneous. It also results clear that ignition time is extremely dependent on the oxidizer temperature and oxygen concentration in regime 2 whilst the dependence on oxidizer properties is significantly reduced in regime 3 and practically eliminated in regime 1, at least if the temperature of the oxidizer is sufficiently high (above 873 K).

Three of the used constants (C_4, α, β) include information about the kinetics of the combustion process at ignition. As can be seen in Table 4, the order of reaction with respect to oxygen (α) of 0.13 fitted the data (which in accordance with the reaction orders of 0.1–0.4 previously reported for heterogeneous ignition of non-devolatilised coal [22]). The low value of the corrective constant, C_5 may be due to the fact that gas phase ignition is not accounted for by the formula.

4. Conclusions

Experiments were performed in which coal particle (in pellet form) pellets were inserted into high-temperature ($T_{oxd} = 873$–1273 K) oxidizers with varying oxygen concentrations ($x_{O_2} = 0.05$–1.0).

Clear difference in ignition behavior was observed under the conditions tested.

The temperature inside the particle at the moment of ignition varied with the temperature and oxygen concentration with decreasing ignition temperatures for increasing oxygen concentrations and oxidizer temperatures.

The mass loss at the moment of ignition was inversely dependent on both oxygen concentration and oxidizer temperature.

The ignition behavior under the conditions tested was classified into three well-known ignition mechanisms.

- Sparking ignition by heterogeneous oxidation of the non devolatalised coal for high-oxidizer temperatures and medium to high-oxygen concentrations.
- Flaming ignition by homogeneous ignition of volatiles for high-oxidizer temperature and low-oxygen concentrations.
- Glowing surface ignition by heterogeneous oxidation of char for low-oxidizer temperature and low-oxygen concentrations.

By comparing the rates of the involved reaction, a theory for the delimitation of ignition mechanism regimes in the oxygen concentration–oxidizer temperature plane was formulated.

Ignition time followed the trends on the solid temperature at the moment of ignition in function of oxygen concentration and oxidizer temperature, but the dependence was even more pronounced.

A formula for the estimation of the ignition time from the oxidizer temperature, oxygen concentration and the material properties was proposed and validated with experimental data. The formula showed that ignition time decrease with increasing oxidizer temperature and increasing oxygen concentration and indicated that the influence of oxidizer temperature and oxygen concentration were the smallest at high-oxidizer temperature.

References

[1] Wünning JA, Wünning JG. Flameless oxidation to reduce thermal NO-formation. Prog Energ Combust Sci 1997;23(12):81.
[2] Hasegawa T, Mochida S, Gupta AK. Development of advanced industrial furnace using highly preheated air combustion. AIAA J Propul Power 2002;2(18):233.
[3] Cavaliere A, de Joannon M. Mild combustion. Prog Energ Combust Sci 2004;30(4):329.
[4] Tsuji H, Gupta AK, Hasegawa T, Katsuki M, Kishimoto K, Morita M. High-temperature air combustion: from energy conservation to pollution reduction. New York: CRC Press; 2003.
[5] Gupta AK, Bolz S, Hasegawa T. Effect of sir preheat temperature and oxygen concentration on flame structure and emission. J Energ Resour Technol 1999;121:209.
[6] Lille S, Blasiak W, Jewartowski M. Experimental study of the fuel jet combustion in high temperature and low-oxygen content exhaust gases. Energy 2005;30:373.

[7] Dally BB, Riesmeier E, Peters N. Effect of fuel mixture on moderate and intense low-oxygen dilution combustion. Combust Flame 2004;137(4):418.

[8] Yang W, Blasiak W. Chemical flame length and volume in liquefied propane gas combustion using high-temperature and low-oxygen concentration oxidizer. Energ Fuel 2004;18:1329.

[9] Coelho PJ, Peters N. Numerical simulation of a mild combustion burner. Combust Flame 2001;124:503.

[10] Yang W, Blasiak W. Flame entrainment induced by a turbulent reacting jet using high-temperature and oxygen-deficient oxidizers. Energ Fuel 2005;19(4):1473.

[11] Blasiak W, Narayanan K, Yang W, von Schéele J. Flameless oxyfuel combustion for fuel consumption and nitrogen oxides emissions reduction and productivity increase. J Energ Inst 2007;80(1):3.

[12] http://www.linde-gas.com/international/web/lg/com/likelgcomn.nsf/docbyalias/ind_rebox.

[13] Lucas C, Szewczyk D, Blasiak W, Mochida S. High-temperature air and steam gasification of densified biofuels. Biomass Bioenerg 2004;29(6):563.

[14] Yougn L, Pian CCP. High-temperature, air-blown gasification of dairy-farm wastes for energy production. Energy 2003;28:655.

[15] Yoshikawa K. In: Proceedings of the 19th annual international Pittsburgh coal conferences, September 2002, Pittsburgh, PA. Paper No. 31-2.

[16] Ponzio A, Kalisz S, Blasiak W. Effect of operating conditions on tar and gas composition in high-temperature air/steam gasification (HTAG) of plastic containing waste. Fuel Process Technol 2006;87:223.

[17] Pian CCP, Yoshikawa K. Development of a high-temperature air-blown gasification system. Bioresource Technol 2001;79:231.

[18] Yang W, Ponzio A, Lucas C, Blasiak W. Performance analysis of a fixed-bed biomass gasifier using high-temperature air. Fuel Process Technol 2006;87:235.

[19] Orsina S, Tamura M, Stabat P, Constantini S, Proado O, Weber R. Excess enthalpy combustion of coal. IFRF Doc. No. F46/y/3, IJmuiden, January; 2000.

[20] Kiga T, Yoshikawa K, Sakai M, Mochida S. Characteristics of pulverized coal combustion in high-temperature preheated air. J Propul Power 2000;16(4):601.

[21] Suda T, Takafuji M, Hirata T, Yoshino M, Sato J. A study of combustion behavior of pulverized coal in high-temperature air. P Combust Inst 2002;29:503.

[22] Essenhigh RH, Misra MK, Shaw DW. Ignition of coal particles: a review. Combust Flame 1989;77:3.

[23] Kuo JT, His C-L. Pyrolysis and ignition of single wooden spheres heated in high-temperature streams of air. Combust Flame 2005;142:401.

[24] Faraday M, Lyell C. Explosions in coal mines. Philos Mag 1845;26:16.

[25] Wheeler RV. In United Kingdom explosion in mines committee. 2nd report. London: HMSO; 1912. 4th report; 1913.

[26] Chen Y, Mori S, Pan W-P. Studying the mechanisms of ignition of coal particles by TG-DTA. Thermochim Acta 1996;275:149.

[27] Faúndez J, Arenillas A, Rubiera F, García X, Gordon AL, Pis JJ. Ignition behaviour of different rank coals in an entrained flow reactor. Fuel 2005;84:2172.

[28] Grotkjær T, Dam-Johansen K, Jensen AD, Glarborg P. An experimental study of biomass ignition. Fuel 2003;82:825.

[29] Gururajan VS, Wall TF, Gupta RP, Truelove JS. Mechanisms for the ignition of pulverized coal particles. Combust Flame 1990;81:119.

[30] Hull AS, Agarwal KP. Estimation of kinetic rate parameters for coal combustion from measurement of the ignition temperature. Fuel 1998;77:1051.

[31] Molina A, Shaddix CR. Ignition and devolatilisation of pulverized bituminous coal particles during oxygen/carbon dioxide coal combustion. P Combust Inst 2007;31(2):1905.

[32] Wendt JOL. Fundamental coal combustion mechanisms and pollutant formation in furnaces. Prog Energ Combust Sci 1980;6:201.

[33] Yang L, Chen X, Zhou X, Fan W. The pyrolysis and ignition of charring materials under an external heat flux. Combust Flame 2003;133:4007.

[34] Chen M, Fan LS, Essenhigh RH. Prediction and measurement of ignition temperatures of coal particles. Proceedings of twentieth symposium (international) on combustion. Pittsburgh: The Combustion Institute; 1984. p. 1513.

[35] Cassel HM, Liebmann I. The cooperative mechanism in the ignition of dust dispersions. Combust Flame 1959;3:467.